

## Improvement in the performance of solar adaptive optics

Xiao-Fang Zhang<sup>1</sup> and Lian-Qi Wang<sup>2</sup>

<sup>1</sup> School of Optoelectronics, Beijing Institute of Technology, Beijing 100081, China;  
[zhangxfbit@gmail.com](mailto:zhangxfbit@gmail.com)

<sup>2</sup> Thirty Meter Telescope Project, 1111 S. Arroyo Pkwy, Suite 200, Pasadena, California 91105,  
USA; [lianqiw@tmt.org](mailto:lianqiw@tmt.org)

Received 2013 June 27; accepted 2013 September 23

**Abstract** Adaptive optics (AO), which provides diffraction limited imaging over a field-of-view (FOV), is a powerful technique for solar observation. In the tomographic approach, each wavefront sensor (WFS) is looking at a single reference that acts as a guide star. This allows a 3D reconstruction of the distorted wavefront to be made. The correction is applied by one or more deformable mirrors (DMs). This technique benefits from information about atmospheric turbulence at different layers, which can be used to reconstruct the wavefront extremely well. With the assistance of the MAOS software package, we consider the tomography errors and WFS aliasing errors, and focus on how the performance of a solar telescope (pointing toward zenith) is related to atmospheric anisoplanatism. We theoretically quantify the performance of the tomographic solar AO system. The results indicate that the tomographic AO system can improve the average Strehl ratio of a solar telescope in a  $10'' - 80''$  diameter FOV by only employing one DM conjugated to the telescope pupil. Furthermore, we discuss the effects of DM conjugate altitude on the correction achievable by the AO system by selecting two atmospheric models that differ mainly in terms of atmospheric properties at ground level, and present the optimum DM conjugate altitudes for different observation sites.

**Key words:** instrumentation: adaptive optics — atmospheric effects — solar system

### 1 INTRODUCTION

Adaptive optics (AO) is a means for real-time compensation of image degradation caused by atmospheric turbulence (Roddier 1999), and its effect is commonly restricted by atmospheric anisoplanatism (Roddier et al. 1993). The performance of a classical AO system with a single deformable mirror (DM) is usually reduced by a factor of  $\exp\left[-(\theta/\theta_0)^{5/3}\right]$  (Fried 1982), where  $\theta$  is the field of view (FOV), and  $\theta_0$  is the isoplanatic angle defined by Fried (1982). For an optical system with a finite aperture, the fundamental anisoplanatic degradation deviates from the above  $5/3$  power law, including a substantial quadratic region for small angles (Stone et al. 1994). Although under good seeing conditions, the useful FOV is an order of magnitude larger than the field predicted by the isoplanatic angle when using spatially degraded wavefront corrections (Chun 1998), typically an FOV of only a few arcseconds is corrected. This is insufficient for solar observations of sunspots with a size of  $30''$  and the associated active region extending to  $2' - 3'$  (Dong et al. 2012). Multi-Conjugate

Adaptive Optics (MCAO) is a concept that was developed based on turbulence correction by means of several DMs conjugated to different heights, by which the limit of a small corrected FOV that is achievable with AO is overcome and a wider FOV is able to be corrected (Beckers 1988; Johnston & Welsh 1994). Although MCAO has been present for more than 20 years, its application in solar telescopes is still in the initial stage. Due to the complex nature of a wavefront sensor, bad atmospheric seeing, challenges in observations taken at visible wavelengths, a smaller isoplanatic patch and very high bandwidth in a closed loop, the development of an MCAO system is complicated (Berkefeld et al. 2010; Rimmele & Marino 2011).

In solar MCAO, two approaches to wavefront sensing have been implemented: the star-oriented (SO) approach (Tallon & Foy 1990; Ragazzoni et al. 1999) and the layer-oriented approach (Ragazzoni et al. 2000). In the SO approach, light from different points that act as reference stars is used to retrieve the three-dimensional distribution of the phase perturbations in the atmosphere, and tomography can be employed to actuate the DM to correct the distorted image of a scientific target. For solar observations, the Sun, as an extended object, provides an infinite number of references that act as guide stars in any desired geometry, which is especially useful for tomographic reconstruction. One or more correlating Shack-Hartmann wavefront sensors (WFSs) look at the Sun, and a three-dimensional reconstruction of atmospheric perturbations is made. The correction is then applied to one or more DMs. Due to the tomographic reconstruction implying a significant upper layer, the tomographic AO system with a single DM conjugated to the ground enables a reduction in phase variance across the FOV. Moreover, greater reduction in wavefront error is achievable when using more guide stars (Langlois et al. 2004). Due to the complexity of the MCAO system, we focus on the performance of tomographic AO systems with a single DM. Can an AO system with a single DM improve the performance of a solar telescope? The purpose of this paper is to quantify the performance of tomographic solar AO systems. Here we ignore the effects caused by temporal delay, contrast limitation of the source, nonzero FOV of the correlating Shack-Hartmann WFS and solar elevation angle (Marino 2012). We only focus on how the performance of a solar telescope (pointing to zenith) is related to atmospheric anisoplanatism. Typically for solar AO systems, a single DM is conjugated to the ground. In fact, the conjugate altitude of the DM depends on the profile available at different sites.

In this paper, we study the effects of DM conjugate altitude on correction of the AO system by selecting two atmospheric models that differ mainly in terms of their atmospheric properties at ground level, and present the optimum DM conjugate altitudes for different observing sites. In our paper, we simulate the whole process of wavefront sensing and correction in a tomographic solar AO system based on the MAOS software package and evaluate its performance. The remainder of this paper is organized as follows. In Section 2, wavefront reconstruction consisting of wavefront tomography and DM fitting is reviewed. In Section 3, the simulation software MAOS is described, and the two profile models of atmospheric turbulence, based on solar observation, are set up. In Section 4, the performance of a tomographic solar AO system is simulated, and the simulation results are presented.

## 2 WAVEFRONT RECONSTRUCTION

In our tomographic solar AO system, the wavefront reconstruction consists of two steps: atmospheric turbulence tomography and DM fitting.

### 2.1 Atmospheric Turbulence Tomography Reconstruction

Classical modal tomography (Ragazzoni et al. 1999) estimates the coefficients of a Zernike expansion of the wavefront over metapupils defined at different altitudes to reconstruct the wavefront tomography. In our paper, instead of a modal decomposition, the minimum variance wavefront reconstruction (Ellerbroek 2002) based on zonal decomposition is used. The method of atmospheric

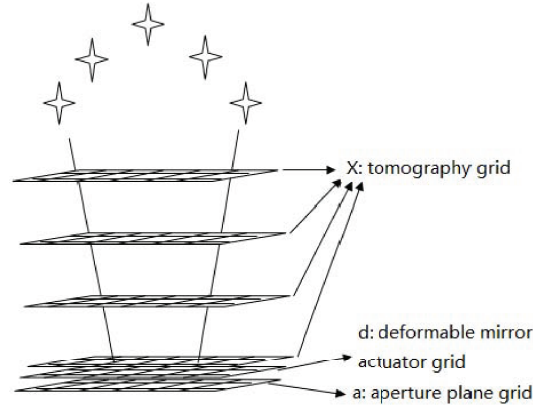


**Fig. 1** Grid for tomography and DM fitting.

tomography has been described by Gilles & Ellerbroek (2008), which consists of computing wavefront values at the intercepts of rays traced through the atmosphere to/from the aperture plane, computing the wavefront gradient from values in the aperture plane, and regularizing the tomography matrix by providing a sparse approximation of the inverse atmospheric covariance matrix. All the above operations are performed on two types of wavefront grids: tomography grids and aperture plane grids. For computational convenience, the two grids are square (see Fig. 1). For a natural guide star (NGS), according to the algorithm described by Ellerbroek (2002), the tomography can be summarized by the following equation,

$$\hat{s} = \left( \tilde{H}_s^T G_a^T C_n^{-1} G_a \tilde{H}_s + C_s^{-1} \right)^{-1} \tilde{H}_s^T G_a^T C_n^{-1} g_{ol}, \quad (1)$$

where  $\hat{s}$  denotes the reconstructed wavefront defined on the tomography grid,  $\tilde{H}_s$  is the ray tracing operator for the NGS beam from the tomography grid to the aperture plane grid,  $G_a$  is the influence function from the aperture plane grid to the gradient of the WFS,  $C_s$  is the covariance of the atmospheric turbulence and  $g_{ol}$  and  $C_n$  are the gradient of the pseudo open loop WFS and covariance of its measurement noise respectively.

## 2.2 DM Fitting

DM fitting is the key issue in AO. Many numerical methods such as the so-called maximum a posteriori (MAP) reconstruction (Le Louarn 2002), classic least squares wavefront reconstruction (Ellerbroek 2002) and minimum variance wavefront reconstruction (Wallner 1983) have been developed, and are used in existing conventional AO systems (Fried 1977; Herrmann 1980; Wallner 1983) and proposed AO or MCAO systems (Tyler 1994; Johnston & Welsh 1994; Fusco et al. 2001). In our paper, utilizing the minimum variance wavefront reconstruction, the DM grids (see Fig. 1) are set up and the DM fitting can be summarized by the following equation,

$$\mathbf{d} = \left( H_d^T W H_d \right)^{-1} H_d^T W H_s \hat{s}, \quad (2)$$

where  $\mathbf{d}$  is the DM command vector,  $H_s$  and  $H_d$  are ray tracing operators from the tomography grid and DM actuator grid, respectively, to the science focal plane grid from the direction of multiple guide stars with the weighting defined by  $W$ .  $\hat{s}$  is the output of Equation (1) describing tomography. The above wavefront reconstructions are implemented in our simulation tool of the MAOS software

(see Sect. 3.1). For minimum variance reconstructions, it is known that sparse matrix methods are not immediately able to be applied. MAOS utilizes a new technique with a sparse approximation for statistics of turbulence to obtain a representation that can be efficiently evaluated using sparse matrix methods for AO systems (Ellerbroek 2002; Wang & Ellerbroek 2012).

### 3 DESCRIPTION OF SIMULATED SOLAR AO

#### 3.1 MAOS

The simulation tool MAOS is software written in C that is a linear AO simulator. It was programmed by one of the authors, Dr. Wang, and can be acquired from <https://github.com/lianqi/maos>. A diagram of how the AO simulation is implemented in MAOS is shown (see Fig. 2). Although it was originally designed for the Thirty Meter Telescope's AO system, the whole process of wavefront sensing and correction can be implemented in a solar AO by developing custom parameters for a solar AO system in conjunction with a telescope. The critical part is rebuilding the atmospheric turbulence models represented by several discrete screens at different heights. These evolve according to the atmospheric structure constant  $C_n^2$  and the wind velocity of classical solar observation sites. The resulting atmospheric aberrations, corrected afterwards by a single DM, are sensed by correlating Shack-Hartmann WFSs. In MAOS, the sensors are either simulated as idealized wavefront gradient sensors, tip-tilt sensors based on the best Zernike fit, or a WFS using physical optics and incorporating user specified pixel characteristics and a matched filter pixel processing algorithm. The tomographic wavefront reconstruction described in Section 2 then estimates the turbulence at several different heights from the pseudo open loop gradients measured by the WFS, using a minimum variance reconstruction algorithm. These reconstructed screens representing turbulence are then fit to the actuators on a single DM to achieve the best possible correction over a specified FOV.

Based on MAOS, we simulate the whole wavefront sensing and correction process in a tomographic solar AO system and analyze its performance. Moreover, we build two atmospheric models to study the effects of DM conjugate altitude applied to the AO system correction for different observing sites and present the optimum DM conjugate altitudes which are consistent with the derived theoretical values.

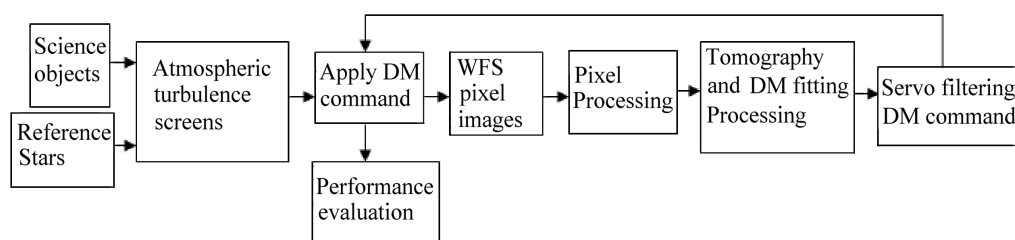


**Fig. 2** Diagram showing simulations of the AO system in MAOS. The atmospheric turbulence is represented as one or several discrete screen(s) at different heights that evolve according to the atmospheric structure constant  $C_n^2$  and wind velocity. The resulting aberrations, after being corrected by one DM, are sensed by one or more Shack-Hartmann wavefront sensors that use multiple natural guide stars. The tomographic wavefront reconstruction then estimates the turbulence from the pseudo open loop gradients measured by the wavefront sensor. These reconstructed turbulence screens representing turbulence are then fitted and the result is applied to the actuators on one DM to achieve the best possible correction over a specified FOV.

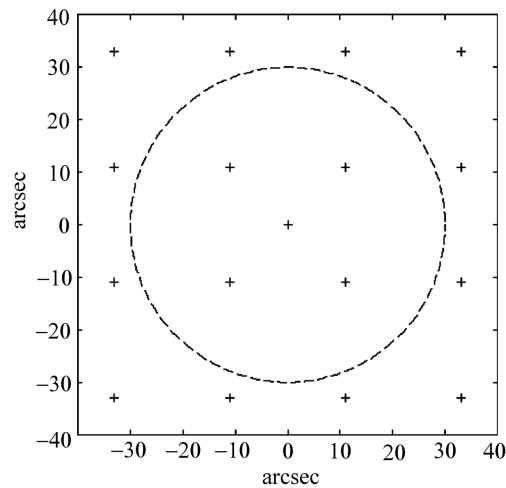


**Fig. 3** Profile of 17 guide stars for a  $60''$  FOV. The point '+' is the position of every point that acts as a guide star. 17 points obtained from the solar structures are located on the solar disk, with 16 of them placed at equal intervals over the  $60''$  diameter FOV and one at the center. In order to ensure the field used for evaluating the system's performance (the circle indicated by a dashed line) is smaller than the reference field that the stars cover, we make the latter become bigger than  $60''$  in diameter.

### 3.2 Guide Stars

It is well known that the number or geometry of guide stars will affect the performance of AO systems (Fusco et al. 1999; Femenía & Devaney 2003). The Sun is the ideal target for tomography, and any number of points that act as guide stars can be made from the structure of the Sun by using a correlating WFS. In our simulation, we suppose that 17 points obtained from solar structures are located on the solar disk; 16 of them form a grid on the FOV, and one is at the center. As an example, the distribution of points acting as guide stars for a  $60''$  diameter FOV is shown (see Fig. 3), in which the point '+' is the position of every guide star.

Due to the 17 guide stars giving sufficient sky coverage to sense the wavefront across the  $5''$ – $80''$  diameter FOV, we can use the geometry of the above guide stars for convenience in the simulation.

### 3.3 Evaluation of Performance of the Tomographic Solar AO System

Based on MAOS, performance evaluation is done in terms of the Strehl ratio (SR) of a few science objects in the target FOV. We put  $3 \times 3$  science objects at equal intervals into the target FOV to calculate SRs, and then the mean of SRs is used to evaluate the performance of the tomographic solar AO system, which is defined as the "average SR" in our paper. As an example, evaluation of the performance over an FOV with a diameter of  $60''$  is shown (see Fig. 3; the circle indicated by the dashed line is the evaluation of the performance in the FOV).

In order to focus on how the performance of the solar telescope (pointing to zenith) is related to atmospheric anisoplanatism, only tomography errors and WFS aliasing errors are considered. Other factors, such as temporal delay, DM fitting errors, WFS noise and reconstruction error, are considered to be zero.

### 3.4 Generation of Atmospheric Turbulence

In order to study the performance of the solar AO system for different observing sites, we select two classical turbulence profiles that differ mainly in terms of atmospheric properties at ground level. We determine a suitable turbulence model by computing simulated profiles of  $C_n^2(h)$  according to the actual coherence length  $r_0$  of turbulence in daytime conditions.

#### 3.4.1 Atmospheric turbulence model 1: with a strong ground atmosphere

We consider the Hufnagel-Valley (H-V) model (Hill et al. 2003) as an example of a vertical profile, which is well-known and often cited.

The H-V profile is an equation that relates atmospheric altitude  $h$  to  $C_n^2$

$$C_{nHV}^2(h) = A_{HV} \left[ 2.2 \times 10^{-23} \left( \frac{h+z}{1000} \right)^{10} \exp\left(-\frac{h+z}{1000}\right) \times \frac{7}{21} + 10^{-16} \exp\left(-\frac{h+z}{1500}\right) \right], \quad (3)$$

where  $A_{HV}$  is a chosen amplitude,  $z$  is the elevation of the site in meters, and the average wind velocity is  $7 \text{ m s}^{-1}$ . We consider a solar observation on a mountain which has a strong ground atmosphere, and suppose the elevation is 2800 m, which is a typical value based on the National Solar Observatory (NSO) at Sacramento Peak.

The H-V model is a good approximation to  $C_n^2(h)$  for nighttime conditions. For a better model of  $C_n^2(h)$  during the daytime, we add an additional profile near the ground

$$C_n^2(h) = C_{nHV}^2(h) + A_B \exp\left(-\frac{h}{h_0}\right), \quad (4)$$

where  $A_B$  is the boundary amplitude and  $h_0$  is the boundary scale height, which is 100 m.

Taking the NSO-Sacramento Peak as the observation site, the actual turbulence coherence length  $r_0$  in daytime and nighttime are 0.07m and 0.15m respectively. We calculated the amplitude  $A_{HV}$  and  $A_B$ , and constructed the simulated profiles as follows

$$C_n^2(h) = 8.0546 \times \left[ 2.2 \times 10^{-23} \left( \frac{h+z}{1000} \right)^{10} \exp\left(-\frac{h+z}{1000}\right) + 10^{-16} \exp\left(-\frac{h+z}{1500}\right) \right] + 9.0560 \times 10^{-15} \exp\left(-\frac{h}{100}\right). \quad (5)$$

The first atmospheric model, with a strong ground atmosphere, is based on the  $C_n^2(h)$  profile simulation obtained from Equation (5).

#### 3.4.2 Atmospheric turbulence model 2: with a weak ground atmosphere

We take the European Northern Observatory (ENO) located on the Island of Tenerife as an observing site to construct an atmosphere model with a weak ground atmosphere because of the excellent quality of the sky. Still based on the H-V model, with the additional profile near the ground being ignored, the derived  $C_n^2(h)$  profile can be described as follows. Here the coherence length  $r_0$  of turbulence in daytime conditions is supposed to be 0.15 m.

$$C_n^2(h) = 4935.5 \times \left[ 2.2 \times 10^{-23} \left( \frac{h+z}{1000} \right)^{10} \exp\left(-\frac{h+z}{1000}\right) + 10^{-16} \exp\left(-\frac{h+z}{1500}\right) \right]. \quad (6)$$

The second atmospheric model, with a weak ground atmosphere, is based on the profile simulation  $C_n^2(h)$  obtained from Equation (6).

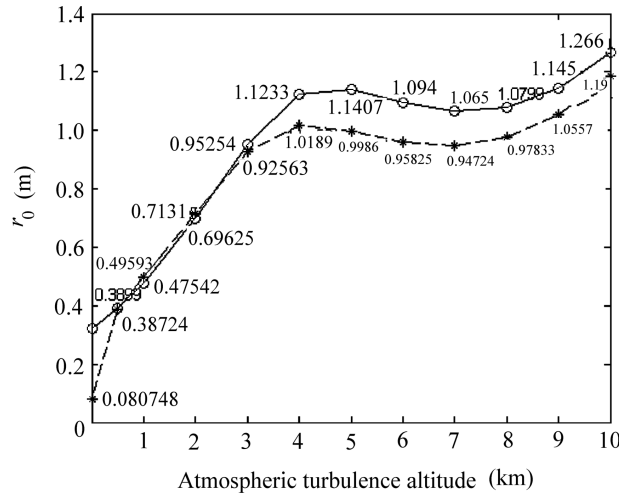


**Fig. 4** Profiles of  $r_0$  from 0 to 10 km according to atmospheric model 1 and model 2 obtained from Eqs. (5) and (6). The atmospheric turbulence from 0 to 10 km is separated into 12 layers, having heights of 0, 0.5, 1, 2, 3, 4, 5, 6, 7, 8, 9 and 10 km respectively. The values of  $r_0$  related to each layer are noted in the '\*' (atmospheric model 1) or 'o' (atmospheric model 2) symbols along the curves.

In this paper, by using Equation (5) and Equation (6), the  $r_0$  of discrete turbulence layers for the two atmosphere models can be calculated. We assume that the atmospheric turbulence from 0 to 10 km is separated into 12 layers, having heights of 0, 0.5, 1, 2, 3, 4, 5, 6, 7, 8, 9 and 10 km respectively. Then the profiles of  $r_0$  from 0 to 10 km for the two atmosphere models are shown (see Fig. 4). In addition, the isoplanatic angles  $\theta_0$  can be calculated, and their values are 2.74'' and 2.99'' respectively.

It is not our intention, with our choice of atmospheric models, to compare the quality of different observing sites. Our aim is to study the impact that turbulence will have on the correction performance of a solar AO system. We selected the atmospheric profiles to be used in the AO simulations as examples of atmospheres with general characteristics of turbulence in solar observations.

#### 4 SIMULATION RESULTS

For solar AO systems, one of the main problems is to increase the corrected FOV, which is typically 1 arcmin in the visible. The limitation in the compensated FOV is mainly related to the height of the turbulence layers. It occurs because of differences between wavefronts coming from different directions. This is called anisoplanatism and is evaluated by the so-called isoplanatic angle  $\theta_0$ . Due to solar observations being done at low elevations,  $\theta_0$  decreases as the 6/5 power of wavelength and -8/5 power of air mass, which makes the performance of solar AO drop with an increasing FOV. Using SR to evaluate the performance of a solar AO system, the decrease in the SR related to anisoplanatism is described as a function of compensated FOV

$$SR_{\text{decrease}} \propto \exp \left[ - (\theta/\theta_0)^{5/3} \right], \tag{7}$$

where  $\theta$  is the compensated FOV, and  $\theta_0$  is the isoplanatic angle.

It is clear that the above conclusion is limited to the case of infinite aperture size, but  $\theta_0$  is still widely used because it is independent of the system and permits easy comparisons between various sites (Tokovinin et al. 2000). In the tomographic AO system, atmospheric tomography is regarded as

a way to measure three dimensional phase perturbations in the atmosphere. Due to the tomographic reconstruction implying a significant upper layer, the AO system with a single DM enables an improvement in SR across the FOV. Below, we simulate the performance of the tomographic solar AO system. In order to focus on how the performance of the solar telescope (pointing to zenith) is related to atmospheric anisoplanatism, we ignore the effects caused by temporal delay, contrast limitation of the source, nonzero FOV of the correlating Shack-Hartmann WFS and solar elevation angle.

Although a single DM is conjugated to the ground in a typical AO system, the DM conjugate altitude depends on the  $C_n^2(h)$  profile at different sites. We simulate the effects of DM conjugate altitude on correction of the AO system by using two atmospheric models (see Sect. 3.3) that differ mainly in terms of atmospheric properties at ground level, and present optimum DM conjugate altitudes for different observing sites.

All simulations are based on the MAOS software package. Focusing on anisoplanatism, only tomography errors and WFS aliasing errors are considered. To evaluate the performance of the tomographic solar AO system, the average SR of a few science objects in the target FOV is calculated.

#### 4.1 Performance of a Tomographic Solar AO Employing one DM Conjugated to the Telescope Pupil

In order to quantify the performance of the tomographic solar AO employing one DM conjugated to the telescope pupil, we consider a model of a solar telescope with a 1.6 m diameter and a 500 nm observation wavelength. As any number of points that act as guide stars can be acquired from the disk of the Sun, 17 guide stars with geometry described in Section 3.2 are adopted that can be sensed by correlating WFSs. The three dimensional perturbations caused by atmospheric turbulence model 1 (with  $r_0 = 0.07$  m) are reconstructed and are then employed to actuate the DM to correct the scientific target in a certain FOV. The average SR across a different FOV is used to evaluate the performance of the tomographic solar AO system.

In Table 1, we remove the piston and tip-tilt errors because solar images are transmitted through, insensitive to these effects.

**Table 1** Average SRs across different FOVs for solar AO with or without tomography.

FOV (arcsec)	Average SR (AO with tomography)	SR (AO without tomography)
0	0.99	1
5	0.79	0.48
10	0.6	0.1
15	0.47	0.01
20	0.38	$5.8 \times 10^{-4}$
25	0.31	$2.1 \times 10^{-5}$
30	0.26	$4.5 \times 10^{-7}$
40	0.20	$5.6 \times 10^{-11}$
50	0.18	$1.3 \times 10^{-15}$
60	0.17	$6.9 \times 10^{-21}$
70	0.16	$8.6 \times 10^{-27}$
80	0.14	$2.8 \times 10^{-33}$

Figure 5 shows the performance of a tomographic solar AO system ( $D/r_0 \approx 23$ ) employing one DM conjugated to the telescope pupil. Moreover, according to Equation (7), the theoretical performance of how AO is related to isoplanatism without tomography ( $(\theta/\theta_0)^{5/3}$  law) is also shown (see Fig. 4) to compare with that of a tomographic solar AO system.

As shown in Figure 5, using enough guide stars, a tomographic solar AO system with only one DM (no MCAO) can greatly improve the performance of a solar telescope with an FOV of  $10''$  –

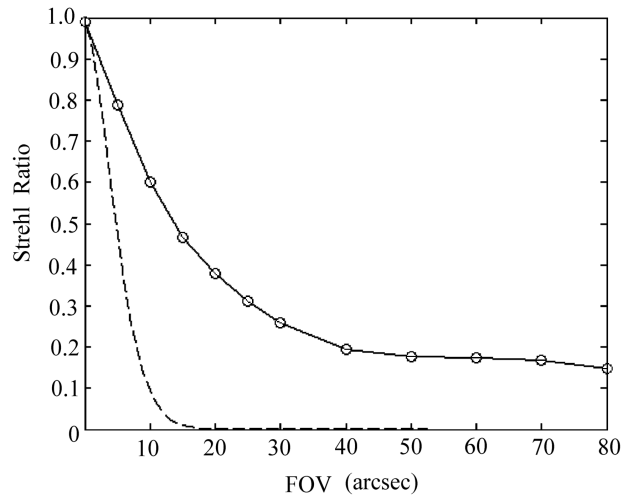


**Fig. 5** The solid line indicates the performance (that is the average SR in different FOVs) of an AO system employing one DM conjugated to the telescope pupil. The diameter of the solar telescope is 1.6 m, and the observational wavelength is 500 nm. Adopting 17 guide stars and the atmospheric turbulence  $C_n^2(h)$  profile based on Eq. (5), three dimensional perturbations are reconstructed and are then employed by a DM to correct the scientific target in a certain FOV. The dashed line indicates how the theoretical performance of an AO system is related to isoplanatism without tomography ( $(\theta/\theta_0)^{5/3}$  law).

80'' in diameter. Many authors have noted that the performance of an AO system is better than the process of modeling anisoplanatism (Chassat et al. 1989; Stone et al. 1994; Chun 1998). Without tomography, the corrected FOV of a low-order AO system is 1.5–2 times larger than the atmospheric isoplanatic angle  $\theta_0$  (Tokovinin et al. 2001). In our simulation, despite neglecting the piston and tip-tilt errors, the effect of a tomographic reconstruction on the performance of AO is still significant. Tomographic reconstruction offers better estimation of the total atmospheric turbulence, especially in the upper layer. This can be utilized to employ a single DM to improve the performance of a solar telescope. As shown in Figure 5, for a tomographic AO system ( $D/r_0 \approx 23$ ), the average SR of this kind of system can be increased by hundreds of times. In theory, based on a tomographic reconstruction, the limit of the small corrected FOV that is achievable with classical AO is overcome and a wider FOV (about 10'' – 80'') is corrected by utilizing an AO system. The average of SR of a tomographic AO system across a corrected FOV with a diameter of 25'' reaches 0.3 (after removing the piston and tip-tilt errors). This indicates that the corrected FOV of an AO system is five times larger than the atmospheric isoplanatic angle  $\theta_0$ .

Moreover, the degradation of SR varies slightly in an FOV of 40'' – 80'', which indicates that the corrected FOV should theoretically be expanded further based on tomographic reconstruction.

In Figure 5, due to the temporal delay, DM fitting error, WFS noise and reconstruction errors being zero, the theoretical SR (removing the piston and tip-tilt errors) of a 0'' FOV is approximately 1.0. Based on MAOS, we calculate the on-axis SR in 20'', 30'', 40'', 50'' and 60'' corrected FOVs. With an increasing FOV, the on-axis performance drops, which is shown in Figure 6. The on-axis performance is sacrificed for an increased FOV, but compared with that of the theoretical performance of AO related to isoplanatism without tomography ( $(\theta/\theta_0)^{5/3}$  law), the average performance of the total FOV is modified (see Fig. 5).

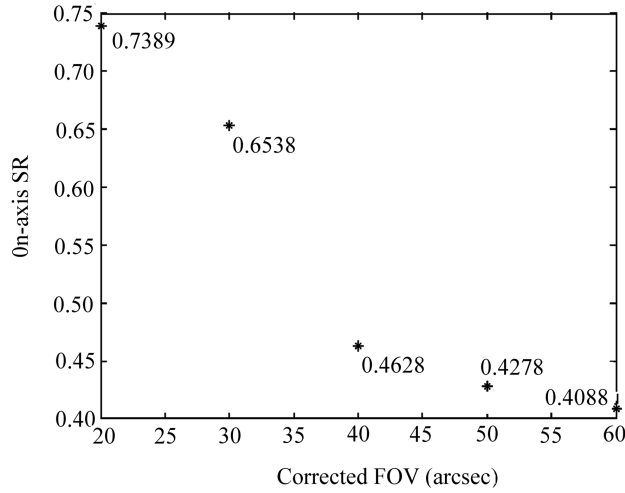


**Fig. 6** The values of on-axis SR are denoted as “\*”, which indicate the on-axis performance of a tomographic AO system employing one DM conjugated to the telescope pupil in the corrected FOV of 20”, 30”, 40”, 50” and 60”. The diameter of the solar telescope is 1.6 m, and the observational wavelength is 500 nm. 17 guide stars and the atmospheric turbulence profile  $C_n^2(h)$  based on Eq. (5) are adopted.

## 4.2 Optimum DM Conjugate Altitude

Ignoring the effect of geometry and number of guide stars (Femenía & Devaney 2003), the optimum conjugate altitude of a DM depends on the profile according to different sites. Despite the existence of the theoretical calculation of the DM conjugate altitude (Tokovinin et al. 2000), the issue of optimum DM conjugate altitude for a solar tomographic AO system is still not clear. Based on tomographic reconstruction, we deduce the optimum conjugate altitude of a DM for a solar AO system. With the help of MAOS, we simulate the effects of DM conjugate altitude on correction in an AO system using two atmospheric models (see Sect. 3.3). These differ mainly in terms of the atmospheric properties at ground level, and show the optimum DM conjugation altitudes for different observing sites, which are consistent with the derived theoretical values.

### 4.2.1 Theoretical optimum DM conjugate altitude

In an AO system, the residual phase variance depends on many parameters associated with the system. Considering a system-independent characteristic related to isoplanatism, the residual phase variance (Tokovinin et al. 2000) can be written as,

$$\langle \text{error}^2 \rangle = 2.905k^2|\theta|^{5/3} \int_0^{h_{\max}} C_n^2(h)|h - H|^{5/3} dh, \quad (8)$$

where  $k = 2\pi/\lambda$  is the optical wave number,  $\theta$  is the half angle of the FOV,  $h$  is the altitude of atmospheric turbulence, and  $H$  is the conjugate altitude of a DM. For a tomographic AO system, considering the tomographic reconstruction, Equation (8) can be changed to

$$\langle \text{error}^2 \rangle = 2.905k^2|\theta|^{5/3} \sum_n C_n^2(h_n)|h_n - H|^{5/3}, \quad (9)$$

where  $n$  is the number of discrete turbulence layers in the atmospheric model, and  $h_n$  is the altitude of the  $n$ th atmospheric turbulence.

Equation (9) reflects the fact that for on-axis viewing, the atmospheric turbulence can be corrected by a DM with any conjugate altitude. Also, for off-axis viewing, in order to minimize the residual phase variance, the optimum DM conjugate altitude, depending on atmospheric turbulence profile  $C_n^2(h)$ , can be described as

$$\langle \text{error}^2 \rangle_{\min} = 2.905k^2 |\theta|^{5/3} \sum_n C_n^2(h) |h_n - H_{\text{opt}}|^{5/3}, \quad (10)$$

where  $\langle \text{error}^2 \rangle_{\min}$  denotes the minimum residual phase variance, and  $H_{\text{opt}}$  is the optimum conjugate altitude of a DM.

#### 4.2.2 Simulation of the Optimum DM conjugate altitude

Equation (10) is derived from the limiting case of infinite aperture size. Can it be applied in a tomographic solar AO system with finite aperture? Below, based on MAOS, we select the solar telescope model described in Section 4.1 to simulate the effects of a DM conjugate altitude in correction of an AO system using two atmospheric models (see Sect. 3.3). We compare the simulation of optimum DM conjugate altitudes with theoretical values calculated by Equation (10).

Figure 7 and Figure 8 show the residual phase variance across the corrected FOV (with diameters  $5''$ ,  $20''$  and  $40''$ ) of a tomographic solar AO system employing one DM with different conjugate altitudes under atmospheric turbulence model 1 (with  $r_0 = 0.07$  m) and model 2 (with  $r_0 = 0.15$  m)

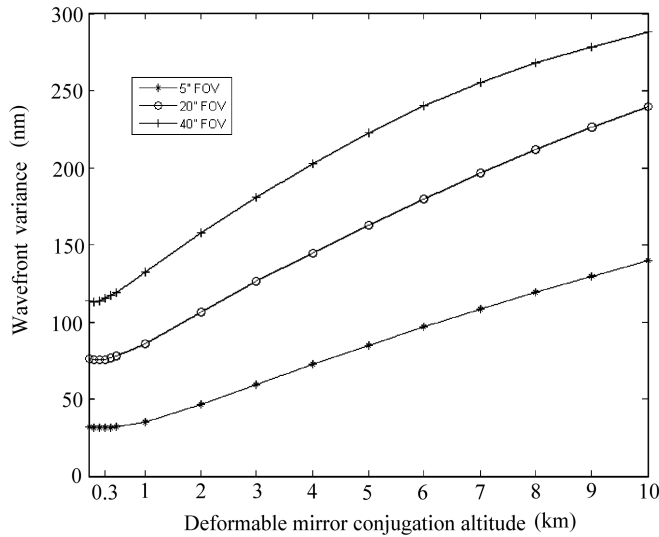


**Fig. 7** The wavefront variance of a solar AO system employing one DM with different conjugate altitudes (from 0 to 10 km) after the piston and tip-tilt errors are removed. The atmospheric turbulence profile  $C_n^2(h)$  is based on Eq. (5). The diameter of the solar telescope is 1.6 m, and the observational wavelength is 500 nm. Adopting 17 guide stars and the atmospheric model with 12 turbulent layers, three dimensional perturbations are reconstructed and are then employed to actuate a DM to correct the scientific target in a certain FOV. Three curves represent results for corrected FOVs of  $5''$ ,  $20''$  and  $40''$  respectively.

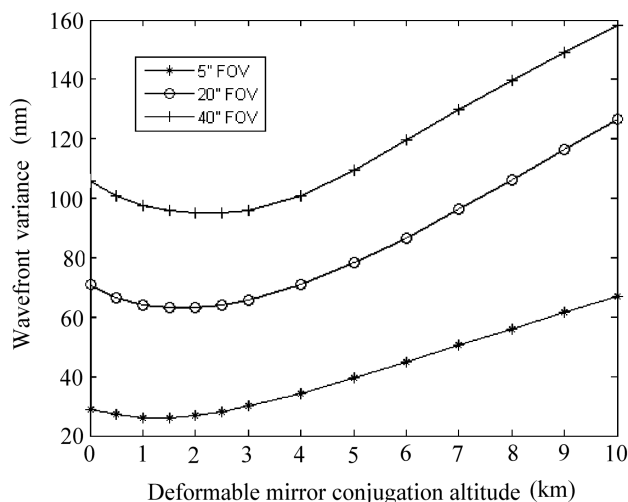


Fig. 8 The same as Fig. 7, but  $C_n^2(h)$  is based on Eq. (6).

respectively. The optimum DM conjugate altitude depends strongly on the atmospheric turbulence profile  $C_n^2(h)$ , and varies slightly with a change of the FOV. For atmospheric turbulence model 1, the optimum DM conjugate altitude is 0–300 m, and the performance of a tomographic solar AO system with a DM placed at 0–300 m produces optimum results with performance varying by only a few of nanometers root mean square (RMS) for different FOVs. Similarly, for atmospheric turbulence model 2, the optimum DM conjugate altitude is 2000–2500 m for different FOVs.

Substituting Equations (5) or (6) into Equation (10), optimum conjugate altitudes of a DM under the above atmospheric models can be calculated. For atmospheric model 1, the optimum conjugate altitude of a DM is 300 m, and for model 2, it is 2200 m. This is consistent with values from the simulation. The optimum conjugate altitude of a DM can be estimated from Equation (10), which offers the conjugate altitude of a DM for a real solar AO system.

With increasing FOV, the effect of optimum conjugate altitudes for a DM on the performance of an AO system becomes more significant in agreement with  $\theta^{5/3}$ , according to Equation (10). Considering the effect of conjugate altitudes of a DM, the residual phase variance caused by a non-optimum DM conjugate altitude across a corrected FOV of  $40''$  is about 1.5 times larger than that of  $5''$ .

As shown in Figure 7 and Figure 8, although the optimum DM conjugate altitudes are different according to the profiles  $C_n^2(h)$  at different sites, the performance of an AO system with DM placed from pupil to optimum conjugate altitude varies by only a few tens of nanometers RMS for different FOVs. For a real solar AO system with only a single DM, despite the difference in the  $C_n^2(h)$  profile for different sites, the DM can always be conjugated to the pupil, which has little effect on the performance of an AO system.

## 5 CONCLUSIONS

The Sun, as an extended object, can provide an infinite number of points that act as guide stars in any geometry, which is especially useful for an AO or MCAO. In our paper, using 17 guide stars and a model with an atmosphere having 12 layers of turbulence, based on a tomographic reconstruction, the performance of an AO employing one DM is simulated. Focusing on anisoplanatism,

only tomographic errors and WFS aliasing errors are considered. The simulation results show that a tomographic AO system ( $D/r_0 \approx 23$ ) can greatly increase the average SR of a solar telescope with a  $10'' - 80''$  diameter FOV even by only employing one DM conjugated to the telescope pupil. The average SR of a tomographic solar AO system across the corrected diameter FOV of  $25''$  reaches 0.3 (after removing the piston and tip-tilt errors), which indicates that the corrected FOV of a tomographic AO system is five times larger than the atmospheric isoplanatic angle.

In this paper, we theoretically deduce the optimum DM conjugate altitude. With the help of MAOS, we simulate the effects of DM conjugate altitude on correction by the AO system by using two atmospheric models that differ mainly in terms of atmospheric properties at ground level. These present the optimum DM conjugation altitudes for different observing sites, which are consistent with the derived theoretical values. Moreover, with an increasing FOV, the effect of optimum conjugate altitudes of a DM on the performance of a tomographic AO system becomes more significant. Generally, for a real solar AO system, despite the difference in observing sites, a single DM can always be conjugated to the pupil, which has little effect on the performance of an AO system.

It must be noted that the above conclusions are only valid in an ideal situation. For a real AO system, the performance will be reduced by temporal delay, limitations in contrast of the source, nonzero FOV of the correlating Shack-Hartmann WFS, solar elevation angle, DM errors, etc. However, the results presented in our paper should play an important role by directing research about a real solar AO system.

**Acknowledgements** The China Scholarship Council Foundation is acknowledged for funding this research.

## References

- Beckers, J. M. 1988, in European Southern Observatory Conference and Workshop Proceedings, 30, Increasing the Size of the Isoplanatic Patch with Multiconjugate Adaptive Optics, ed. M.-H. Ulrich, 693
- Berkefeld, T., Soltau, D., Schmidt, D., & von der L uhe, O. 2010, Applied Optics, 49, G155
- Chassat, F., Rousset, G., & Primot, J. 1989, in Society of Photo-Optical Instrumentation Engineers (SPIE) Conference Series, 1130, New Technologies for Astronomy, ed. J.-P. Swings, 33
- Chun, M. 1998, PASP, 110, 317
- Dong, B., Ren, D.-Q., & Zhang, X. 2012, RAA (Research in Astronomy and Astrophysics), 12, 465
- Ellerbroek, B. L. 2002, Journal of the Optical Society of America A, 19, 1803
- Femen a, B., & Devaney, N. 2003, A&A, 404, 1165
- Fried, D. L. 1977, Journal of the Optical Society of America (1917–1983), 67, 370
- Fried, D. L. 1982, Journal of the Optical Society of America (1917–1983), 72, 52
- Fusco, T., Conan, J.-M., Michau, V., Mugnier, L. M., & Rousset, G. 1999, in Society of Photo-Optical Instrumentation Engineers (SPIE) Conference Series, 3763, Propagation and Imaging through the Atmosphere III, eds. M. C. Roggemann, & L. R. Bissonnette, 125
- Fusco, T., Conan, J.-M., Rousset, G., Mugnier, L. M., & Michau, V. 2001, Journal of the Optical Society of America A, 18, 2527
- Gilles, L., & Ellerbroek, B. L. 2008, Journal of the Optical Society of America A, 25, 2427
- Herrmann, J. 1980, Journal of the Optical Society of America (1917–1983), 70, 28
- Hill, F., Radick, R., & Collados, M. 2003, ATST Site Survey Working Group Final Report. ATST Proj. Doc, 14
- Johnston, D. C., & Welsh, B. M. 1994, Journal of the Optical Society of America A, 11, 394
- Langlois, M., Moretto, G., Richards, K., Hegwer, S., & Rimmele, T. R. 2004, in Society of Photo-Optical Instrumentation Engineers (SPIE) Conference Series, 5490, Advancements in Adaptive Optics, eds. D. Bonaccini Calia, B. L. Ellerbroek, & R. Ragazzoni, 59
- Le Louarn, M. 2002, MNRAS, 334, 865

- Marino, J. 2012, *Optical Engineering*, 51, 101709
- Ragazzoni, R., Farinato, J., & Marchetti, E. 2000, in *Society of Photo-Optical Instrumentation Engineers (SPIE) Conference Series*, 4007, *Adaptive Optical Systems Technology*, ed. P. L. Wizinowich, 1076
- Ragazzoni, R., Marchetti, E., & Rigaut, F. 1999, *A&A*, 342, L53
- Rimmele, T. R., & Marino, J. 2011, *Living Reviews in Solar Physics*, 8, 2
- Roddier, F. 1999, *Adaptive Optics in Astronomy* (1st ed.; Cambridge: Cambridge Univ. Press)
- Roddier, F., Northcott, M. J., Graves, J. E., McKenna, D. L., & Roddier, D. 1993, *Journal of the Optical Society of America A*, 10, 957
- Stone, J., Hu, P. H., Mills, S. P., & Ma, S. 1994, *Journal of the Optical Society of America A*, 11, 347
- Tallon, M., & Foy, R. 1990, *A&A*, 235, 549
- Tokovinin, A., Le Louarn, M., & Sarazin, M. 2000, *Journal of the Optical Society of America A*, 17, 1819
- Tokovinin, A., Le Louarn, M., Viard, E., Hubin, N., & Conan, R. 2001, *A&A*, 378, 710
- Tyler, G. A. 1994, *Journal of the Optical Society of America A*, 11, 409
- Wallner, E. P. 1983, *Journal of the Optical Society of America* (1917–1983), 73, 1771
- Wang, L., & Ellerbroek, B. 2012, in *Society of Photo-Optical Instrumentation Engineers (SPIE) Conference Series*, 8447, *Adaptive Optics Systems III*, eds., B. L. Ellerbroek, E. Marchetti, & J.P. Véran, (Amsterdam: SPIE), 844723